

ION DETECTION TECHNIQUES APPLIED TO RYDBERG ATOMS IN EXTERNAL FIELDS

F. Penent, C. Chardonnet, D. Delande, F. Biraben and J.C. Gay

Laboratoire de Spectroscopie Hertzienne de l'Ecole Normale Supérieure,
Tour 12 E01, 4, Place Jussieu, 75230 Paris Cedex 05, France*

Résumé - Au cours des cinq dernières années, le développement simultané de l'excitation par laser continu accordable et monofréquence et des méthodes de détection thermoionique a permis de disposer d'une puissante technique expérimentale pour les études en phase vapeur. L'une des applications les plus intéressantes dans le domaine de la physique fondamentale concerne les problèmes ouverts pour lesquels l'atome de Rydberg fournit une base d'étude bien adaptée, par exemple pour l'étude des propriétés de l'atome dans des champs extérieurs. Plusieurs situations choisies sont analysées à la lumière de modèles vectoriels généralisés du diamagnétisme, de l'effet Stark linéaire et du régime en champs électrique et magnétique croisés. Bien que les résultats expérimentaux soient en tous points révélateurs du comportement hydrogénoïde en champs extérieurs, aucun de ces résultats n'a été obtenu sur l'atome d'hydrogène lui-même.

Abstract - The simultaneous development of single mode c.w. dye laser excitation and thermoionic detection over the last five years has supplied with one of the most powerful experimental technique for atomic physics studies under vapour phase conditions. One of the most interesting application concerns problems of fundamental physics which can be tackled on Rydberg atoms especially the ones dealing with the atomic properties in external fields. Several selected examples are discussed to the light of generalized vectorial models of diamagnetism, linear Stark effect and crossed electric and magnetic fields effects. Although the experimental results are highly illustrative of the pure hydrogenic behaviour in external fields, none of them have been obtained on the hydrogen atom itself.

Applying an external field on the atom leads to fundamental alterations of the atomic properties /1,2/. For example the atomic spectra may drastically differ from the usual Rydberg type in zero field. In addition, a complete modification of the symmetry properties of the wavefunctions takes place.

Although these questions are somewhat basic ones in physics, they are to some extent unsolved. They have recently received renewed consideration. This is largely in consequence of the development of tunable dye lasers and of our ability of producing and detecting atoms in high Rydberg states.

Regarding those kinds of fundamental problems, the selection of situations in which the atoms behave as hydrogen atoms is worthwhile. This insures that the external field perturbation of the spectra is not hindered by the spurious effects of close range corrections to the Coulomb potential. Hence, the alteration of the atomic spectra due to the external field action can be observed in nearly pure conditions allowing meaningful comparisons with theory in its simplest and most basic form. A way of tending to such an achievement is producing atoms with high n and l values. The higher the (n,l) values, the smaller the departures from the perfect hydrogenic behaviour as the system will tend to behave as an electron tightly bound to an ionic core. Providing a convenient choice of the excitation process, this is a way of producing atoms in Rydberg states having an almost hydrogenic behaviour, but without the complications of dealing with hydrogen atoms.

*associé IA 18

After some elementary recalls on the symmetry properties of the hydrogen atom, we will present some experimental aspects of its spectrum under various conditions of external fields. The emphasis will be on the low field behaviour of the spectrum with discussions of the linear Stark effect, of the rovibrational structure of a diamagnetic manifold and of the atomic spectrum in crossed electric and magnetic field conditions. All these results have been obtained using the technique of thermionic detection with c.w. single mode dye laser excitation in either Doppler-free or non-Doppler free excitation processes. Although those experimental results are illustrative of the hydrogenic behaviour in external fields, none of them have been obtained using hydrogen atoms.

1 - THE HYDROGEN ATOM IN EXTERNAL FIELDS

1.1 - The zero-field Coulomb problem

The most part of the basic aspects of the interaction of an atom with external fields can be understood from an elementary analysis based on the symmetry properties of the Coulomb spectrum in zero field.

The important feature in the Coulomb spectrum is the n^2 degeneracy of each energy level with principal quantum number n , with respect to l and M . On more general grounds, this is associated with the existence of a supersymmetry for Coulomb-like potentials and with the peculiar structure of the symmetry group /3,4/. Indeed a quite convenient description for our present concerns can be derived from arguments of classical physics.

The classical trajectory (the Kepler ellipse) is a closed curve. This means that besides the conservative character of the angular momentum \vec{L} (as in all situations involving centrally symmetric potentials), there must be an additional conservative quantity with vectorial character and directed along the major axis of the Kepler ellipse. This is the well-known Lenz vector \vec{A} , the modulus of which is proportional to the eccentricity of the ellipse /4/. The quantum expression of \vec{A} is just :

$$\vec{A} = \frac{1}{2}(\vec{p} \wedge \vec{L} - \vec{L} \wedge \vec{p}) - me^2 \frac{\vec{r}}{r}$$

with obvious notations. In a given energy shell with fixed principal quantum number n , it is worthwhile introducing a scaled definition of the \vec{A} vector :

$$\vec{a} = (-2mH)^{-1/2} \vec{A} \quad (1)$$

where H is the hamiltonian. One then gets :

$$\vec{a}^2 + L^2 + h^2 = -me^4/2E = n^2 h^2 \quad (2)$$

$$\vec{a} \cdot \vec{L} = 0$$

The (\vec{a}, \vec{L}) vectors allow a complete description of the Coulomb spectrum and of the degeneracies in a given energy shell n . Indeed, it is much more convenient to deal with the new set of operators :

$$\begin{aligned} \vec{j}_1 &= (\vec{L} + \vec{a})/2 \\ \vec{j}_2 &= (\vec{L} - \vec{a})/2 \end{aligned} \quad (3)$$

These operators do commute with the hamiltonian in a given energy shell and possess all the properties of two independant angular momenta. They fulfill :

$$j_1^2 = j_2^2 = j(j+1)h^2 \quad (4)$$

$$(2j+1)^2 h^2 = -me^4/2E$$

Hence $n = 2j + 1$ meaning that j is either an integer or an half integer for a given n value. It is then straightforward to derive the eigenfunctions for fixed n value.

A natural choice is that of the uncoupled representation of the two angular momentum $\{j_1^2 j_2^2 j_{1z} j_{2z}\}$ from which it is clear that the degeneracy of the n subshell is n^2 . An equivalent choice is $\{j_1^2 j_2^2 L_z A_z\}$ in which the z components of the angular momentum and of the Runge Lenz vector are defined. Such a choice is associated with the separability of Schrödinger's equation in parabolic coordinates. A third possible description is through the coupling scheme $\{j_1^2 j_2^2 (j_1 + j_2)^2 (j_1 + j_2)_z\}$ or $\{j_1^2 j_2^2 L^2 L_z\}$ which is associated with the familiar description through spherical

harmonics. Of course, the passing from one basis to the other one only involves Clebsch-Gordan coefficients /5/.

From such a description follows a vectorial model of the hydrogen atom recalled on Figure (1).

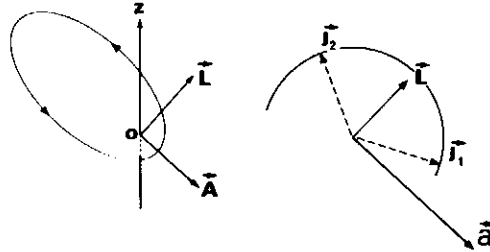


Fig. (1) - Vectorial model of the Hydrogen atom.

1.2 - Hydrogen atoms in external fields. Generalized vectorial models

a) External electric field - Linear Stark effect

Under such conditions, the system is well-known /6/ to be separable in parabolic coordinates which in turn is associated with the existence of an exact dynamical symmetry /3,6/. We restrict the analysis to a given energy shell. The adiabatic invariant is then the energy of interaction with the external field \vec{E} :

$$W = q \vec{E} \cdot \vec{r} \quad (5)$$

From classical perturbation theory, $\langle \vec{r} \rangle$ is proportional to \vec{A} . Then, one gets (in atomic units) (the \vec{E} field is directed along z axis) :

$$W = \frac{3}{2} n^2 \vec{A} \cdot \vec{E} = \frac{3}{2} n (j_{1z} - j_{2z}) E \quad (6)$$

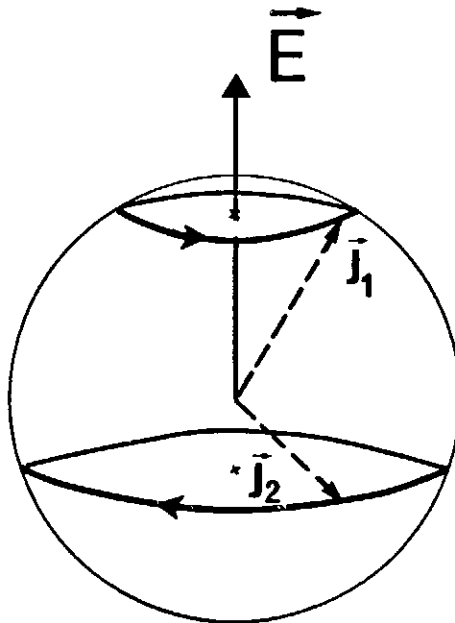


Fig. (2) - Stark vectorial model at low fields.

Another constant of the motion is the projection of the angular momentum on the field axis :

$$L_z = (j_{1z} + j_{2z}) \quad (7)$$

Then, from (6) and (7), the n^2 degeneracy of the shell is partially removed by the introduction of the electric field. The manifold is splitted into $2n - 1$ components,

with a spacing $\frac{3}{2} n E$. Such a quantity ω_E

$$\omega_E = \frac{3}{2} n E \quad (8)$$

is the linear Stark frequency associated with the precession of \vec{j}_1 and \vec{j}_2 around \vec{E} (see Figure (2)). Then, Stark effect is a linear phenomenon for the hydrogen atom at low fields. The eigenfunctions are obviously of the $\{j_1^2, j_2^2, j_{1z} - j_{2z} = q, j_{1z} + j_{2z} = M\}$ types. Writing

$$n = n_1 + n_2 + |M| + 1 \quad (9)$$

$$A_z = (n_1 - n_2) / n$$

one recovers the usual description in terms of the parabolic quantum numbers $(n_1, n_2) / 6/$. From (6) each component $q = n_1 - n_2$ in the manifold presents a $n - |q|$ degeneracy in the M value.

This perturbative description is valid provided $\frac{1}{n^3} \gg \omega_E = \frac{3}{2} n E$ that is for field values smaller than the critical ionisation field $/1/$.

b) Symmetries in an external magnetic field. Paramagnetism and diamagnetism

The interaction hamiltonian with the magnetic field is composed of two parts $/2,5/$

$$W = -\frac{qB}{2m} L_z + \frac{q^2 B^2}{8m} (x^2 + y^2) \quad (10)$$

The first term (linear in B field) is responsible for the usual orbital Zeeman effect and associated with paramagnetism (\vec{L} precesses around the \vec{B} field at Larmor frequency ; see Figure (3)).

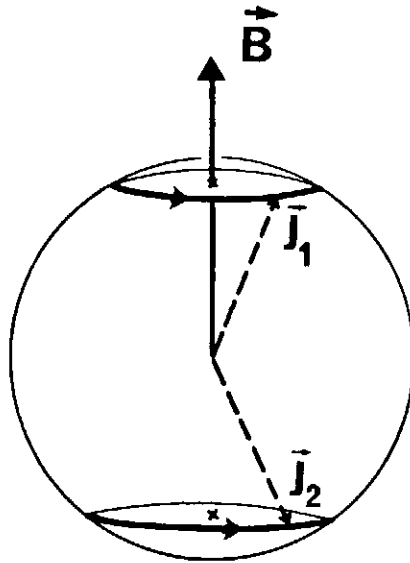


Fig. (3) - Vectorial model of paramagnetism

The second term (quadratic in B field) is called diamagnetic interaction. It is often negligible for low-lying states, but it can be important for high Rydberg states.

In contrast to the previous situation, there is no exact dynamical symmetry. The projection L_z of the angular momentum onto the \vec{B} field axis is conserved

$$L_z = j_{1z} + j_{2z} = M \quad (11)$$

A correct description of the interaction (including the diamagnetic one) was performed for the first time in 1981 /7,8/ in the low field regime.

As in the electric field case, an adiabatic invariant Λ can be derived in terms of the \vec{j}_1 and \vec{j}_2 operators. From the invariance of the diamagnetic interaction under various spatial transformations, its expression can be shown to involve only terms as j_{1j_2} and $j_{1z}j_{2z}$ /9/, while the derivation of the coefficients can be done choosing simple situations of quantum or classical physics /9/. One gets exactly

$$\Lambda = 3n^2 + 1 - 4M^2 + 4(5j_{1z}j_{2z} - 2\vec{j}_1\vec{j}_2) \quad (12)$$

while the complete expression of the energy in such conditions becomes (in atomic units)

$$E = -\frac{1}{2n^2} + \frac{\gamma M}{2} + \frac{\gamma^2}{16} n^2 \Lambda \quad (13)$$

with $\gamma = \hbar\omega_c/2Ryd$ the reduced magnetic field ($\omega_c = qB/m$ is the cyclotron frequency) From (12), it is clear that the diamagnetic interaction involves an unusual coupling scheme of the two angular momenta \vec{j}_1 and \vec{j}_2 /5,8/. Then, it can be shown that the symmetry of the diamagnetic manifold is of rovibrational type.

For each M value, the manifold is splitted into about $n/2$ components due to the diamagnetic interaction. When $\gamma n^3 \approx 1$, the previous analysis breaks down, and the atomic Rydberg spectrum evolves to a Landau type spectrum /2,10/, that is the spectrum of a free electron in a magnetic field.

c) Symmetries in crossed electric and magnetic fields

Usually, there is no remaining constant of the motion. Nevertheless, if the diamagnetic interaction is negligible, the atomic spectrum is still organized. This manifests the existence of a new class of motion, intermediate between Zeeman and linear Stark effects /11/.

This is readily seen from the expression of the energies :

$$W = \frac{q}{2m} \vec{B} \cdot \vec{L} + q\vec{r} \cdot \vec{E} \quad (14)$$

introducing the (\vec{j}_1, \vec{j}_2) operators and the $\vec{\omega}_L$ (Larmor) and $\vec{\omega}_E$ (Stark) frequencies, one gets (atomic units) :

$$W = (\omega_L + \omega_E) \vec{j}_1 + (\omega_L - \omega_E) \cdot \vec{j}_2 \quad (15)$$

$$\text{Writing } \vec{\Omega}_1 = \omega_L + \omega_E \quad (16)$$

$$\Omega = (\omega_L^2 + \omega_E^2)^{1/2} = \left(\frac{\gamma^2}{4} + \frac{9}{4} n^2 E^2\right)^{1/2}$$

where Ω is the modulus of $\vec{\Omega}_1$ and $\vec{\Omega}_2$, one gets :

$$W = \Omega(j_{1\Omega_1} + j_{2\Omega_2}) \quad (17)$$

The manifold is then splitted into $(2n - 1)$ components which do present a remaining degeneracy. The spacing between two adjacent components is proportional to Ω . Then, in this intermediate regime, the spacing is neither proportional to B nor to E .

The wavefunctions are of $(j_1^2, j_2^2, j_{1\Omega_1}, j_{2\Omega_2})$ types associated with the independent quantizations of j_1 and j_2 along the $\vec{\Omega}_1$ and $\vec{\Omega}_2$ axis. The associated vectorial model is shown on figure (4).

When the \vec{E} and \vec{B} fields are not crossed to each other, the degeneracies are completely removed and the manifold is splitted into n^2 components.

Other types of regimes, where the diamagnetic interaction is not negligible, in high field conditions, have been predicted /12,13,14/. These will not be discussed here.

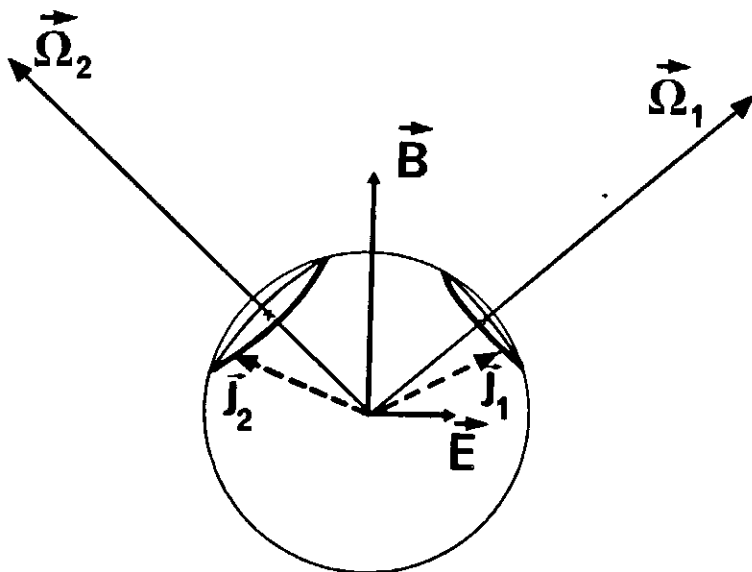


Fig. (4) - Vectorial model of the spectrum in crossed electric and magnetic fields

1.3 - Validity of the analysis for many electron atoms

The previous results are intimately associated with the supersymmetry of the Coulomb problem. For non hydrogenic atoms, this constitutes the basis of the analysis, provided the role of quantum defects is not too important. This means that one will asymptotically recover the ideal hydrogenic situation when :

$$\frac{2R}{n^3} \cdot \delta \ll W$$

where W is the external field perturbation and δ the quantum defect. Practically, this means that one must choose experimental situations in which the atomic behaviour is looking like that of hydrogen, or finding some tricks for checking the part of the spectrum behaving as in hydrogen.

2 - EXPERIMENTAL EVIDENCE OF NEW QUANTIZATION LAWS IN THE SPECTRUM OF MANY ELECTRON ATOMS IN EXTERNAL FIELDS

2.1 - Main characters of the experimental studies

The excitation of high lying Rydberg series of alkali atoms is performed through the use of a c.w. single mode ring dye laser. It delivers about 800 mW power in the 5 900 Å region. This is presently the only class of experiments centered on external field studies of the Rydberg spectrum using such kinds of c.w. dye laser excitation. The laser linewidth is in the range of 1 MHz. The laser line is locked on an external cavity. This allows continuous scans of the frequency on a 150 GHz range without any mode jumps while the lineshape is always perfectly controlled.

Experiments are performed under vapour phase conditions using either Doppler limited excitation schemes equivalent to stepwise excitation or two-photon Doppler free techniques. The detection of Rydberg atoms is performed through the use of a thermionic detector which is basically a space charge limited diode allowing an efficient amplification of the ions produced from the Rydberg atoms. A typical arrangement is shown on Figures 5 and 6. The fact that the method is extremely efficient is well-known and recalled in the following. But the detection is also extremely reliable in the sense that the stray electric fields are well controlled and smaller than 20 mV/cm (depending on the geometry of the detector). Collisions effects inhe-

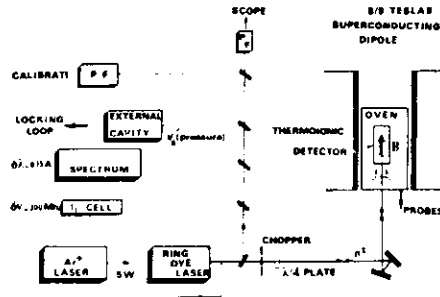


Fig. (5) - Experimental apparatus

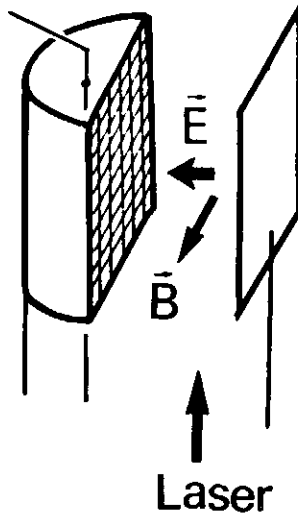


Fig. (6) - Thermoionic detector for crossed (\vec{E}, \vec{B}) fields experiments.

rent to any vapour phase studies are always negligible.

An important advantage of experiments under vapour phase conditions lies in the possibilities of choosing "exotic" excitation schemes leading to the selection of states with almost hydrogenic behaviours. For example, the use of the so-called hybrid resonance process /15,16/ in caesium vapour allows, through absorption of two non-resonant photons, to populate nF Rydberg series. These series with small ($\delta = 0.0335$) quantum defects are almost hydrogenic ones. They are particularly convenient for external field studies with Doppler resolution. The selection of Doppler free two-photon processes on Rb atoms allows on the other hand studies in extremely good conditions of resolution although the nS or nD series are strongly non hydrogenic. As shown below, finding some tricks allows anyway to study the hydrogenic part of the spectrum, although under indirect conditions.

2.2 - The field free Rydberg spectrum

The efficiency of the excitation - detection process is illustrated in zero-field conditions in Figures(7) and (8) /17,18/.

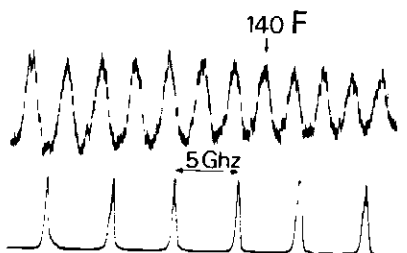


Fig. (7) - Doppler limited Rydberg spectrum (Caesium F series).

Figure (7) displays the Rydberg spectrum of Caesium got using the two-photon hybrid resonance process. Such plots have been obtained for n up to 162 /19/ which is the ultimate value one can expect using Doppler limited techniques. Indeed the Doppler width being of the order of 1 GHz, it is of the order of the spacing $2R/n^3$ between adjacent Rydberg lines for $n \sim 170$. For $n \sim 140$, the collisional shift of the lines is of about 200 MHz (collisional red shift).

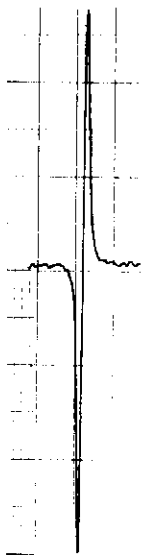


Fig. (8) - Doppler free spectrum (Rb atoms $n=37S$ two-photon line)

2.3 - The quasi-hydrogenic diamagnetic manifold of Caesium

As discussed in §1.2 the action of a magnetic field on the spectrum is two-fold. Firstly the paramagnetic interaction is responsible for the well-known Zeeman effect, linear in B field. Secondly, the diamagnetic interaction proportional to $B^2 \rho^2$ causes a deeper alteration of the spectrum which evolves from Coulomb to Landau type. Such transition has been experimentally studied in great details /17/ especially demonstrating the existence of a new quantization law $n^3 \gamma = 1.56$ obeyed at the zero-field threshold (γ is the reduced magnetic field ; see § 1.2.b) and the evolution of the spectrum from a bound state Rydberg to a Landau resonances spectrum /21,22,23/.

One of the most interesting regime at low fields is the diamagnetic regime in which, due to the break-down of L^2 as a good quantum number, a "forbidden line structure" appears in the excitation spectrum. Such a spectrum is shown in Figures(9).and (10) as a function respectively of the laser frequency and of the B field /17,19/. The situation is that of $M = 3$, odd parity, quasi-hydrogenic states of Caesium. Compared to the pure hydrogenic situation, there are still some small perturbations in the

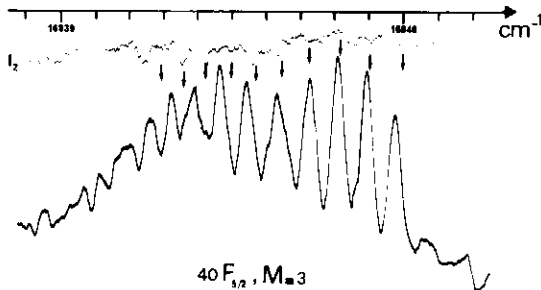


Fig. (9) - Diamagnetic manifold in energy (Caesium M=3 odd parity states) (B = 6.16kG)

oscillator strengths due to the very small quantum defect of the F state. At fixed magnetic field values, the spacing between successive components is just proportional to B^2 . The manifold has about $n/2$ components. To each component is associated a value of the quantum number K which in turn is quantizing the spectrum of the invariant A in formula (12). The states with the smaller K values are located at the top of the diamagnetic band. They are analogous to the states of the oblate spheroidal top with some rotational symmetry (see § 1.2.b). States at the bottom of the band do have vibrational symmetry along the B field axis. The structure of the manifold is then of rovibrational type. A complete description of its properties can be found in references /5,24,25/.

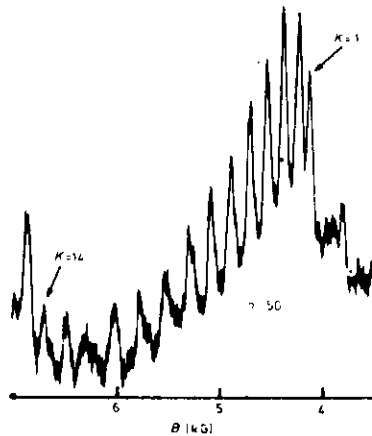


Fig. (10) - Diamagnetic manifold in B field (Cs M=3 odd parity states) at fixed laser frequency

In the previous high field experiment, the field was produced by the means of a super-conductive solenoid and the manifold was checked for low $n \sim 40$ values. The same kind of phenomena will occur at low fields in the range of 500 Gauss provided one is able to produce states with n up to 150, in a Doppler-free experiment. This is under current investigation, and quite clear to understand as the diamagnetic interaction is scaling as $n^4 B^2$.

2.4 - Substructures in the quasi-Landau spectra close to the zero field threshold

In the previous situation, the diamagnetic hamiltonian H_D was a small perturbation of the Coulomb binding energy, that is $2R/n^3 \gg H_D$. Its main role was breaking the supersymmetry in the Coulomb manifold in a well controlled way described in § 1.2.b. But other situations may exist for higher n or field values in which H_D becomes comparable or even greater than the Coulomb binding energies. These regimes are called quasi-Landau and Landau regimes. The first one takes place near the zero field threshold /2,17,22/. It is characterized with the existence of equally spaced resonances (with a spacing $3/2\hbar\omega_c - \omega_c$ the cyclotron frequency) while the quantization law in field, at constant energy of the electron is $n^3 \cdot B = 1.56 \cdot B_c$ ($B_c = 2.35 \cdot 10^9$ Gauss). Although the dominant structures in the spectrum are now well understood /17,23/, it is quite clear that they present substructures as shown on Figure (11). This is an experimental spectrum obtained at threshold on $M = 3$, odd parity quasi-hydrogenic Caesium states. Compared to the situation at low fields discussed in § 1.2.b, the theory is here far from being achieved. But the existence of these substructures can be thought as due to an excited vibrational motion of the electron along the B field axis while dominant structures are associated with the radial quantization of the motion in the direction perpendicular to the field. The quasi-Landau spectrum is then band structured. A simple model allows to show that at threshold, the vibrational spacing is about one fourth of the radial one ($1.5\hbar\omega_c$) which is sufficient for rendering chaotic the general appearance of the spectrum. A numerical si-

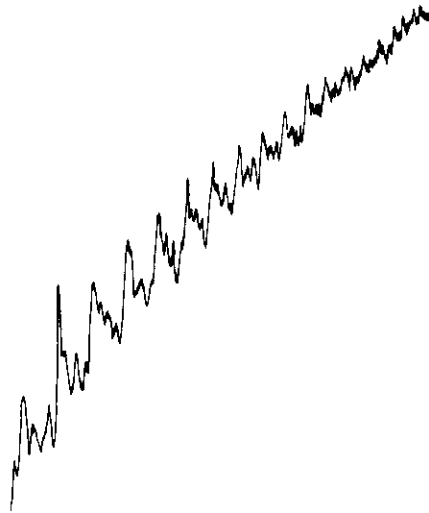


Fig. (11) - Quasi-Landau spectrum at threshold (zero energy of the electron) as a function of the B field strength.

mulation shown on Figure (12) reproduces quite well (at least qualitatively) the features of the experimental spectrum at threshold /19,26/.

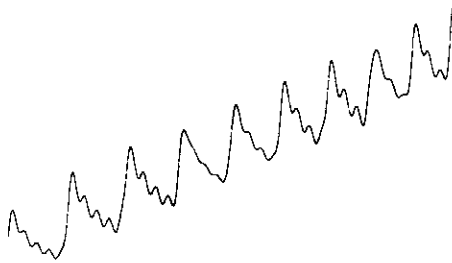


Fig. 12 - Numerical simulations of the quasi-Landau spectrum at threshold (based on a fully 3 dimensional semi-classical analysis)

More generally, such a regime shares numerous common characters with phenomena involving the dynamics of coupled anharmonic oscillators as in intramolecular energy transfer (classical resonance regions) and photochemistry /2,27/.

2.5 - The quasi-hydrogenic Stark manifold

A convenient choice of the electrode arrangements in the detector allows to apply a small electric field in the interaction volume where the atoms are excited /28,29/. In order to avoid any excitation of discharges, the strengths of the field are necessarily small ones. This is not a limitation as a proper choice of the n va-

lue will make the interaction with the external field comparable or even greater than the Coulomb interaction. Furthermore a proper choice of the states under consideration and of the n value allows to get a situation as hydrogenic as possible. That is the role of quantum defects becomes energetically negligible compared to the external fields effects. Then Stark effect will become a linear phenomena at low fields as in the purely hydrogenic situation. This is experimentally reported below in two different situations, on Caesium and Rubidium atoms.

2.5.a- Linear Stark effect of quasi-hydrogenic Caesium series

The excitation of Caesium $M = 3$ Rydberg states through the so-called hybrid resonance process has allowed the experimental observation of the linear Stark effect for n values between 30 and 80, at extremely low electric field strengths between 0 and 12 V/cm /29/. The conditions are nearly hydrogenic ones for all the states involved in the Stark mixing process. Indeed the upper bound of the quantum defects corresponds to that of F states ; then it is fairly small and the condition for such an observation :

$$\frac{\delta}{n^3} \ll \frac{3}{2} n(n_1 - n_2) E$$

is easily fulfilled at low electric field values.

These experimental results /29/ are presently the only direct evidence of the linear behaviour got in ultra low electric field conditions (about one thousand times smaller than in reference /30/) using c.w. dye laser excitation in vapour phase conditions. The structure of the hydrogenic $n = 36$, $M = 3$ Stark manifold is displayed in Figure (13) for $E = 11.3$ V/cm. The manifold is splitted into 33 components associated to the values $n_1 = 0$ to $n_1 = 32$ of the parabolic quantum number (or equivalently to the 33 possible quantized values of the z component of the Runge-Lenz vector). The spacing between adjacent components is $3nE$ (in atomic units) and linearly depends on the field strength, as expected . The average extension of the manifold is then of about $3n^2E$.

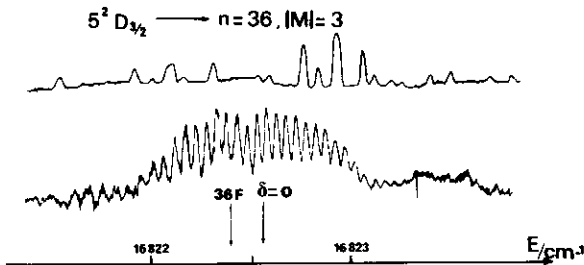


Fig. (13) - Structure of the ($n=36$, $M=3$) linear Stark manifold of Caesium ($E=11.3$ V/cm)

The (n , M , n_1 , n_2) parabolic components of the manifold are manifesting the breaking of the n^2 degeneracy so as to comply with the symmetry of the external electric field perturbation. The previous conditions are such that $1/n^3 \gg 3/2n(n_1 - n_2)E$ so that the successive Stark manifolds are well isolated from each other.

Another aspect of the spectrum is shown on Figure (14) in a regime where several adjacent manifolds are interacting that is the condition $1/n^3 \sim 3/2n(n_1 - n_2)E$ is fulfilled. This is for n around 60 in a range of electric field strengths between 0 and 12 V/cm. Although the manifolds are likely to interact, the energy-field plot of Figure (15) clearly shows that the behaviour of each energy level is still linear in the electric field. Indeed this is the manifestation in a nearly perfect approximation of the existence of a dynamical symmetry in the Stark problem for the hydrogen atom /29/.

There are two kinds of independant contributions in such a plot, associated respecti-

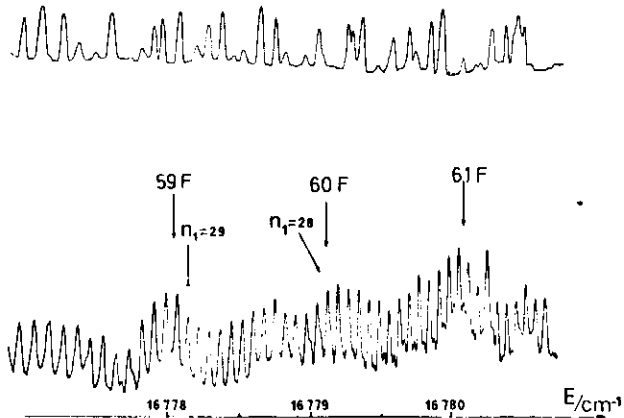


Fig. (14) - Linear Stark spectrum of quasi-hydrogenic $M=3$ Caesium states around $n \approx 60$ ($E = 9.8 \text{ V/cm}$)

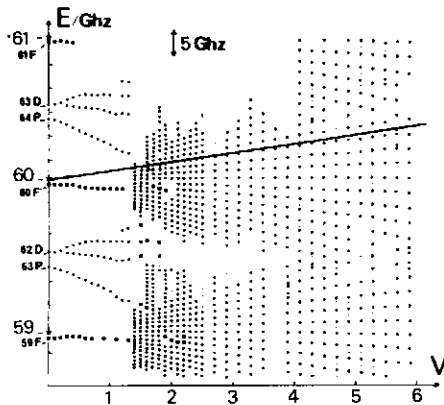


Fig. (15) - Linear Stark plots around $n = 60$ in the inter n mixing regime.

vely with $M = 3$ (quasi-hydrogenic) and $M = 1$ (strongly non-hydrogenic) states, due to some peculiarities of the optical excitation process. The Stark diagram associated with $M = 3$ states only involves states with highly hydrogenic behaviours. This is quite clearly seen from the behaviour of the lines around $n = 59, 60, 61$. Their positions linearly depend on the E field strength on the whole range under investigation. Furthermore, no significant departure from this behaviour occurs in the regime where adjacent manifolds are merging. Individual lines belonging to the various manifolds can still be tracked without any ambiguity. This plot exhibits the linear Stark behaviour as will be seen on the Hydrogen atom, in conditions where the second order term is almost negligible. It is indeed responsible for a systematic quadratic red shift of the position of the lines at maximum of 1 GHz as can be seen on Figure (15).

Of course, the behaviour for non-hydrogenic states, e.g. $M = 1$ states, is completely different /28,29/. But part of the $M = 1$ states, with small quantum defects, will behave as an incomplete linear Stark manifold (see next section). In addition, various classes of quasi-Fano interference profiles manifesting the breaking of the dynamical symmetry due to non-hydrogenic corrections to the potential have been seen on the intensity spectrum /28/.

2.5.b - Doppler-free anticrossing spectroscopy of the linear Stark manifold

The previous experiment allowed a direct investigation of the structure of the linear Stark manifold on quasi-hydrogenic series of Caesium. But we will show here that this is as well possible when dealing with strongly non-hydrogenic states, providing a proper adaptation of the experimental conditions.

The nS , nP and nD series of Rb have important quantum defects (respectively 3.13, 2.65 and 1.35). Consequently, they have a strong non-hydrogenic behaviour when applying an electric field. At low fields, they first exhibit a quadratic Stark effect.

In contrast, states with $l > 3$ (F, G, H... series) have small quantum defects (smaller than $\delta(F) = 0.017$) and are nearly degenerated in zero-field. Consequently, at low fields, they will behave as in the Hydrogen atom situation, exhibiting a linear Stark effect. Such states cannot be excited in a two-photon process from the ground state for $M \geq 3$ states while the states with $M = 2$ and $M = 0$ can be. But they will behave as an incomplete hydrogenic manifold at low fields as the $l = 2$, $l = 1$ and $l = 0$ components are out of the manifold (due to their large quantum defects).

The $M = 0$, $n = 42$ S state exhibits a quadratic Stark effect as shown in Figure (16).

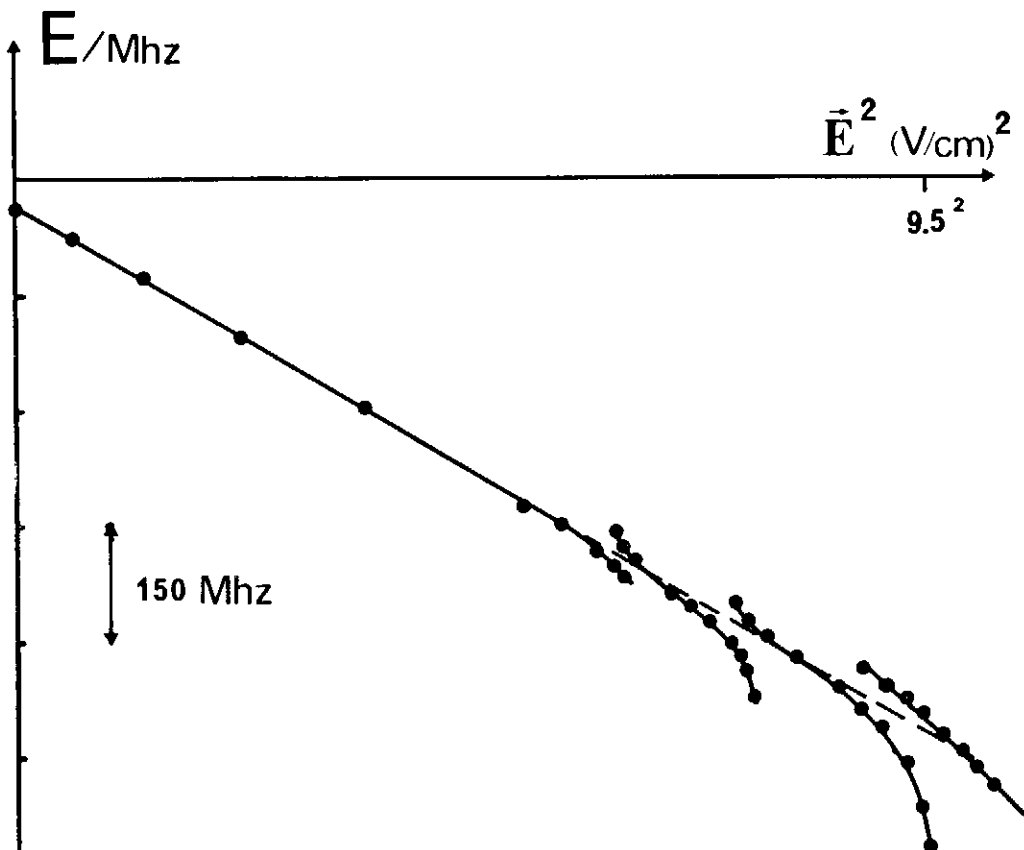


Fig. (16) - Diabolic energy curve of the ($M=0$, $42S$) state of Rubidium (Doppler-free two-photon experiment). The perturbing levels responsible for the anticrossings are those of the incomplete $M=0$ quasi-hydrogenic Stark manifold which linearly behave with the E field.

The energy dependence on the \vec{E} field is a smooth one while the oscillator strength remains concentrated on this line. The coupling between the (nS) and states of the manifold is at third order. The transfer of oscillator strengths is weak. The components of the manifold are not likely to appear on the excitation spectrum except close to the anticrossings points, with the (nS) perturbed state. This is shown in Figure (16). The anticrossings sizes are small, of the order of 100 MHz, as the coupling is weak. A strong but local transfer of oscillator strengths occurs near the crossing. The positions and sizes of the anticrossings are in agreement with theory. The distances between successive crossings are consistent with both a quadratic in \vec{E} behaviour of the energy of the perturbed nS state and a linear in \vec{E} behaviour of the energies of the perturbing levels, issued from the incomplete quasi-hydrogenic Stark manifold. The very weakly depending on the \vec{E} field energy of the nS state is used as a baseline for checking the linear in field quasi-hydrogenic quantization in the manifold /20/.

2.6 - Experimental evidence of a new quantization law in the quasi-hydrogenic manifold, in crossed (\vec{E}, \vec{B}) fields.

The experimental situation on Caesium atoms is suitable for a direct test of the quantization law in the quasi-hydrogenic manifold, in crossed (\vec{E}, \vec{B}) fields. It is under progress. But we are here providing with this evidence on Rubidium atoms using the technique described in § 2.5.b.

The idea is to use the diabatic energy curve of the ($M = 0, nS$) state and its anticrossings with the components of the quasi-hydrogenic manifold so as to check the new quantization which will settle in the manifold, in the presence of a crossed to \vec{E} magnetic field.

In the presence of a \vec{B} field alone, the two photon ($M = 0, nS$) line is splitted into several components associated with the hyperfine structure of the ground state. For fields smaller than 400 Gauss, there are no dependence of the energy on the \vec{B} value as the diamagnetic contribution is still negligible. The energy of the ($M = 0, nS$) state in crossed (\vec{E}, \vec{B}) fields only weakly depends on the \vec{E} field value (quadratically).

But as a consequence of the drastic change of the quantization in the manifold, the positions of the anticrossings will vary with \vec{B} field strength, and compared to the situation in § 2.5.b, new kinds of anticrossings will appear. At high \vec{B} field value the number of anticrossings is twice the number in the absence of \vec{B} field in agreement with the model of § 1.2.c. Such an anticrossing is shown in Figure (17).

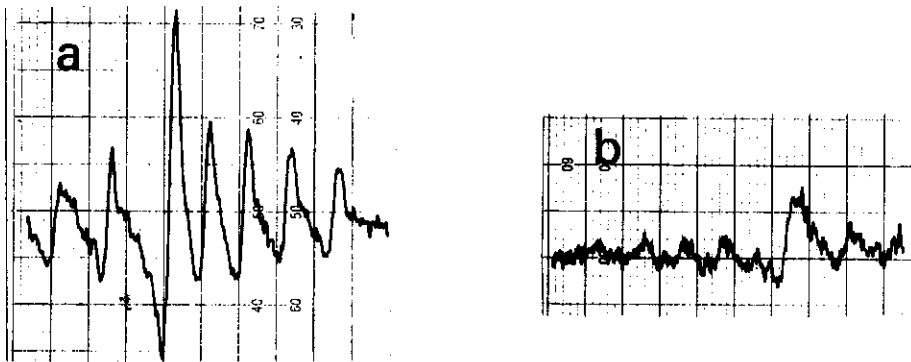


Fig. (17) - Two photons lineshape and anticrossing behaviour in crossed (\vec{E}, \vec{B}) fields ($n = 37S$ transition) - (a) before the anticrossing ($E=6.85$ V/cm ; $B=350$ Gauss) - (b) at the anticrossing ($E=7.08$ V/cm ; $B=350$ Gauss).

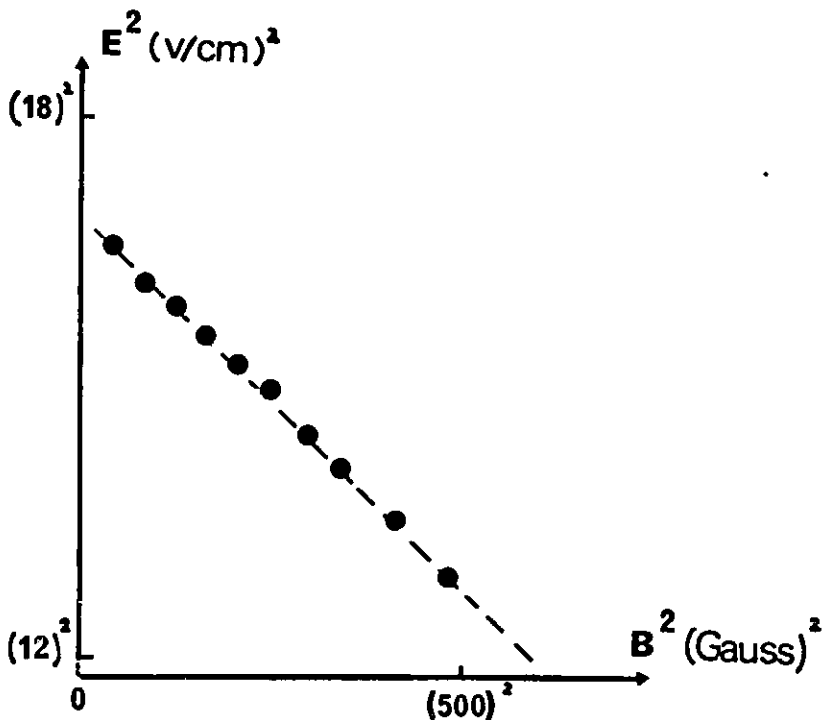


Fig. (18) - Experimental evidence of a new quantization law in crossed (\vec{E}, \vec{B}) fields. As shown in Figure (18), the evolution of the positions of the anticrossings with \vec{E} and \vec{B} just follows a law showing that the spacing is proportional to $[\frac{\gamma^2}{4} + \frac{9}{4} n^2 E^2]^{1/2}$

in agreement with the model of § 1.2.c ($\gamma = B/B_c$ is the reduced magnetic field). This is the first experimental proof of the existence of a new quantization law in the manifold in the regime intermediate between linear Stark effect and Zeeman effect. It is especially clear, as expected, that the distance between successive members of the manifold is neither proportional to B , nor to E , indeed a surprising consequence of the supersymmetry of the Coulomb problem.

3 - CONCLUSION

We have illustrated the usefulness of the thermoionic detection method for dealing with various aspects of the atomic Rydberg spectrum. Contrasting with intuition, it allows accurate determinations of a lot of atomic parameters. Major progresses in atomic physics have been obtained this way, especially as concerns the spectrum in external fields. In this area, the experimental results are presently among the best ever got in extremely varied field strengths and n values conditions. The extension of part of the work towards the production of atoms in states with n around 300 is under progress.

REFERENCES

- /1/ for a review on the electric field problem, see for example S. FENEUILLE and P. JACQUINOT - Ad. At. Mol. Phys. 17 (1981) 99
- /2/ for a review on the magnetic field problem, see for example J.C. GAY in Progress Atomic Spectroscopy - part C (Plenum - 1983 - to be published)
- /3/ B.P. JUDD - Angular Momentum Theory for Diatomic Molecules (Academic Press 1975)
- /4/ M. BANDER and C. ITZYKSON - Rev. Mod. Phys. 38, 330 (1966)
- /5/ D. DELANDE and J.C. GAY - Comments Atomic and Molecular Physics (1983) to be published
- /6/ L.D. LANDAU and E.M. LIFSCHITZ - Mécanique Quantique Ed. MIR (Moscou 1960)
- /7/ E.A. SOLOV'EV - JETP Letters 34 (1981) 265
- /8/ D.R. HERRICK - Phys. Rev. A 26, 323 (1982)
- /9/ D. DELANDE, F. BIRABEN and J.C. GAY - unpublished
- /10/ L.D. LANDAU - Z. Phys. 64 (1930) 629
- /11/ T.P. GROZDANOV and E.A. SOLOV'EV - J. Phys. B 15 (1982) 1195
- /12/ G.P. DRUKAREV and B.S. MONOZON - JETP 34 (1972) 509
- /13/ J.C. GAY, L.R. PENDRILL and B. CAGNAC - Phys. Lett. 72A (1978) 315
- /14/ A.R.P. RAU and K.T. LU - Phys. Rev. A 21 (1980) 1957
- /15/ C.B. COLLINS, B.W. JOHNSON, M.Y. MIRZA, D. POPESCU and I. POPESCU - Phys. Rev. A 10 (1974) 813
- /16/ L.R. PENDRILL, D. DELANDE and J.C. GAY - J. Phys. B 12 (1979) L603
- /17/ J.C. GAY, D. DELANDE and F. BIRABEN - J. Phys. B 13 (1980) L720
- /18/ D. DELANDE and J.C. GAY - Phys. Lett. 82A (1981) 399
- /19/ D. DELANDE - Thèse de 3e Cycle - Paris (1981) unpublished
- /20/ F. PENENT, D. DELANDE, F. BIRABEN and J.C. GAY - Proceedings of the EGAS Conference 1983 (Société Européenne de Physique)
- /21/ D. DELANDE, C. CHARDONNET and J.C. GAY - Optics Comm. 42 (1982) 25
- /22/ W.R.S.GARTON and F.S. TOMKINS - Ap. J. 158 (1969) 839
- /23/ J.C. CASTRO, M.L. ZIMMERMAN, R.B. HULET and D. KLEPPNER - Phys. Rev. Lett. 15 (1980) 1780
- /24/ D. DELANDE and J.C. GAY - Phys. Lett. 82A (1981) 393
- /25/ D. DELANDE, C. CHARDONNET, F. BIRABEN and J.C. GAY - J. Physique (Paris) C2 (1982) 97
- /26/ A.G. ZHILICH and B.S. MONOZON - Sov. Phys. Semicond. 1 (1967) 563
- /27/ J.C. GAY in Photophysics and Photochemistry in the VUV (D. Reidel - N.Y. 1983)
- /28/ C. CHARDONNET - Thèse de 3e Cycle - Paris (1983)
- /29/ C. CHARDONNET, F. PENENT, D. DELANDE, F. BIRABEN and J.C. GAY - J. Phys. Lettres (Paris) - 44 (1983) L517
- /30/ M.G. LITTMAN, M.L. ZIMMERMAN, T.W. DUCAS, R.R. FREEMAN and D. KLEPPNER - Phys. Rev. Lett. 36 (1976) 788.